

## **A Bidirectional Water Reflectance Model with Chlorophyll-*a* Concentration and Backscatter Coefficient as Input**

Park, Young-Je  
Management Unit of the North Sea Mathematical Models (MUMM)  
Royal Belgian Institute for Natural Sciences (RBINS)

### **Introduction**

Correction for bidirectional effects in water reflectance is of increasing importance due to the need for high accuracy in satellite water-reflectance data, e.g. for the inter-comparison of satellite data or for the validation of satellite data with in-situ spectra.

The bidirectional effects depend not only on the viewing and illumination geometry but also on water inherent optical properties (IOPs) such as scattering phase function (SPF), which determines the singly scattered radiance pattern [Morel and Gentili, 1993]. Multiple scattering must also be considered since this modifies the scattered distribution further. The average number of scattering events experienced by a photon exiting water in the viewing direction is determined by the single scattering albedo, which is the ratio of scattering ( $b$ ) to attenuation ( $c=a+b$ , where  $a$ =absorption) [Morel and Gentili, 1991]. For a bidirectional reflectance model to be applicable to satellite remote-sensing data, these effects of SPF and multiple scattering need to be incorporated by variables that can be retrieved from remote-sensing data. This objective has previously been achieved for case 1 waters by the  $f/Q$  factor which is expressed as a function of chlorophyll- $a$  concentration ( $Chl$ ) [Morel and Gentili 1996; Morel et al. 2002]. However, such a model does not apply to more general case 2 waters, where the IOPs such as the SPF and single scattering albedo are a function not only of  $Chl$  but also of non-algae suspended particles and dissolved organic matter. Loisel and Morel [2001] studied the bidirectional structure of water reflectance for two contrasting case 2 water bodies. However, applications of their study are limited to highly scattering or highly absorbing waters.

This study describes a model of the bidirectional water reflectance, applicable to case 1 and case 2 waters. First, the model formulation is given focusing on the model input used to specify the SPF. Second, the radiative transfer simulations made to produce the remote-sensing reflectance ( $R_{rs}$ ) data for the model are described. Third, using the model based on simulation data, the  $R_{rs}$  variability due to the phase function parameters is analysed. Fourth, the model errors are estimated using a different simulated  $R_{rs}$  dataset generated with realistic IOPs. Finally, in the context of practical application to satellite data processing, some remarks on an iterative approach are provided.

### **Model formulation for bidirectional remote-sensing reflectance**

The remote-sensing reflectance above the surface,  $R_{rs}$  is related to the subsurface remote-sensing reflectance,  $r_{rs}$  by the equation, [Gordon et al. 1988]

$$R_{rs} = \left[ \frac{(1-\rho)(1-\bar{\rho})}{n_w^2(1-\bar{r}R)} \right] r_{rs} \quad (1)$$

where  $\rho$  is the surface reflectance for upward radiance;  $\bar{\rho}$  is the surface reflectance for downward irradiance;  $n_w$  is the refractive index of seawater;  $\bar{r}$  is the surface reflectance for diffuse upward irradiance; and  $R$  is the irradiance reflectance just below the surface. The surface interface term (in the square bracket) is determined by sun and sensor angles, surface state (wind), subsurface irradiance reflectance and the angular distribution of the upwelling radiance (which also depends on cloud coverage or aerosol optical thickness). On the other hand,  $r_{rs}$  is strongly dependent on the water inherent optical properties through the factor  $b_b/(a+b_b)$  (or equivalently  $b_b/a$ ). Furthermore, recent studies [Morel and Gentili 1993; Loisel and Morel 2001] on bidirectional properties of  $r_{rs}$  indicate that  $r_{rs}$  varies with SPF and with the number of scattering events a photon undergoes before exiting the ocean surface (multiple scattering effects). Summarising all these, the variables determining  $R_{rs}$  for given sun and sensor angles are the factor  $b_b/(a+b_b)$ , SPF, multiple scattering, wind speed and cloud cover. For simplicity and considering their importance, the first three variables are considered in this study.

In this study, three types of scatterers are considered: pure seawater, phytoplankton and detritus (covarying particles) whose optical properties covary with  $Chl$ , and other non-covarying particles. The average SPF can be approximated by the ratio of particle backscatter to the total backscatter,  $b_{bp}/b_b$  if the particle SPF normalized by backscattering ratio is not highly variable, and this ratio is denoted by  $\gamma_b$  here. By introducing this  $\gamma_b$  parameter as model input, the  $R_{rs}$  model has shown typical errors less than 2% [Park and Ruddick, 2004] when compared with simulated data. However, considering the potentially variable particle mixture e.g. from phytoplankton dominated to non-covarying (terrigenous) particle dominated mixtures, another parameter is necessary for fully specifying the SPF. For this, two extreme particle SPFs,  $P_{FF1}$  and  $P_{FF2}$  (see next section for these phase functions) are considered here and the relative contribution of  $P_{FF1}$  to the particle backscatter,  $r_{FF1}$  ( $=b_{bFF1}/b_{bp}$ ) is introduced as a further model parameter.

Including all variables described above, the following polynomial expansion is adopted for modelling the bidirectional  $R_{rs}$ .

$$R_{rs} = \sum_{i=1}^4 g_i(\theta_o, \theta, \Delta\phi, \gamma_b, r_{FF1}) X^i \quad (2)$$

where  $\theta_o$ ,  $\theta$ ,  $\Delta\phi$  are the angles of solar zenith, sensor zenith and relative azimuth, respectively, and  $X = b_b/(a+b_b)$ . Higher order terms are used for representing multiple scattering effects.

### Scattering phase functions and other simulation input

As mentioned above, particle phase functions are assumed to be represented by a combination of two SPFs,  $P_{FF1}$  and  $P_{FF2}$ . These SPFs have the backscattering to scattering ratio 0.03 and 0.002, respectively. Most measurements lie between these two values [Twardowski et al. 2001]. These two extreme phase functions are given by the Fournier-Forand (FF) analytic expressions [Fournier and Forand, 1994]. A method of selecting the parameter pair, refractive index,  $n_p$  and Junge slope,  $\mu_J$  to fit the backscatter

ratio is described in Mobley et al. [2002].  $P_{FF1}$  and  $P_{FF2}$  are obtained by setting the pair  $(n_p, \mu_j)$  to be (1.117, 3.695) and (1.050, 3.259), respectively. These two FF phase functions are shown in Fig. 1. The SPFs for pure water ( $P_w$ ) and Petzold average particles ( $P_{Petzold}$ ) [Petzold, 1972] are superimposed for comparison. It is notable that the Petzold phase function after normalised to backscatter coefficient cannot be well represented in the backward direction by the FF1 and FF2 phase functions (Fig. 1(b)). This suggests that further study is required for validation of phase functions.

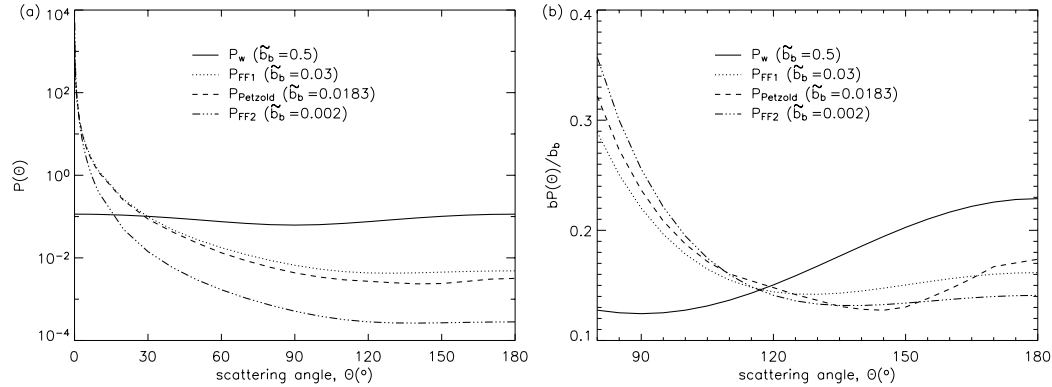


**Figure 1. Scattering phase functions of pure water and particles.**

Radiative transfer simulations were made using Hydrolight 4.2 [Mobley and Sundman 2002] to calculate the remote-sensing reflectance. The water IOPs needed for the simulations are single scattering albedo and average SPF. These are determined by the triplet of variables  $(X, \gamma_b, r_{FF1})$  with the constant SPFs,  $P_w$ ,  $P_{FF1}$  and  $P_{FF2}$ . The input conditions for  $X$ ,  $\gamma_b$ , and  $r_{FF1}$  are:

- $X=0.003, 0.02, 0.04, 0.06, 0.08, 0.1, 0.2, 0.3, 0.4, 0.5$
- $\gamma_b= 0, 0.2, 0.4, 0.6, 0.7, 0.8, 0.9, 0.99$
- $r_{FF1}=0.564, 0.977$

For simplicity, the water is taken to be homogeneous and infinitely deep in the simulations. A cloud free sky and wind speed of 5 m/s are assumed for all simulations. The  $R_{rs}$  are computed for each combination of the sun and sensor angles listed below:

- 7 solar zenith angles: 0, 15, 30, 45, 60, 75, 85°
- 10 sensor zenith angles: 0, 10, 20, 30, 40, 50, 60, 70, 80, 87.5°
- relative azimuth angles: every 15° from 0 to 180°

### Results: model fitting

Using the simulated  $R_{rs}$  data, the coefficients  $g_i$ 's of Eq. (2) are computed and tabulated for discrete values of  $\theta_b$ ,  $\theta$ ,  $\Delta\phi$ ,  $\gamma_b$  and  $r_{FF1}$  described above. Chi-square fitting [Press et al. 1992] was used with the  $R_{rs}$  standard deviation proportional to  $R_{rs}$ .

Figure 2 shows the derived  $R_{rs}$ - $X$  curve for three selected sun and sensor angle combination. An enlarged view for small  $X$  range, 0 to 0.05 is given in the right hand columns. Different line styles indicate different  $\gamma_b$  values. Higher  $\gamma_b$  (higher particle

contribution to backscatter) gives higher  $R_{rs}$  for a given  $X$  except sometimes for small  $X$  as seen in (a') and (b'). More details are given in Park and Ruddick [2004]. Further variability in  $R_{rs}$  for the same  $X$  can be seen when  $r_{FFI}$  varies. Black and red lines are for  $r_{FFI}=0.564$  and  $0.977$ , respectively, with red lines thus corresponding to higher backscattering ratio than black lines. The left hand columns show that larger  $r_{FFI}$  gives lower  $R_{rs}$ . In other words, a larger backscattering ratio for the particle SPF gives lower  $R_{rs}$  for the same  $X$  and  $\gamma_b$ . However, the difference is quite small for small  $X$  and an opposite relationship is shown in (a'). This implies that the impact of  $r_{FFI}$  is more visible when multiple scattering is important. It is noted that the two  $r_{FFI}$  shown in the figure are extreme. In most realistic cases the  $r_{FFI}$  values varies in a more restricted range and thus this  $R_{rs}$  variability due to  $r_{FFI}$  is also limited except for high *Chl* waters.

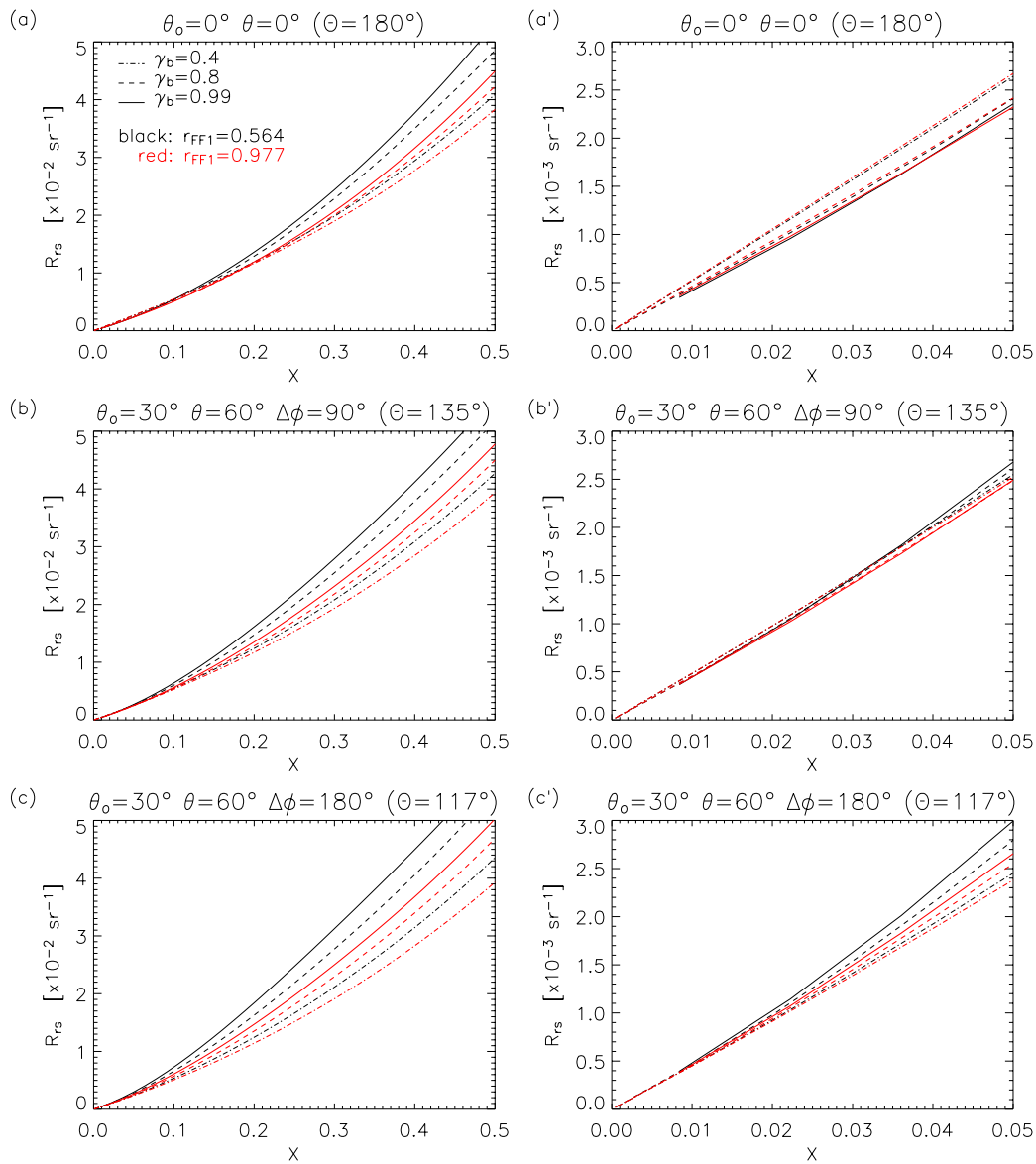


**Figure 2.  $R_{rs}$  versus  $X$ : (a) and (a') for  $\theta_o=0^\circ$ ,  $\theta=0^\circ$ ; (b) and (b') for  $\theta_o=30^\circ$ ,  $\theta=60^\circ$ ,  $\Delta\phi=90^\circ$ ; (c) and (c') for  $\theta_o=30^\circ$ ,  $\theta=60^\circ$ ,  $\Delta\phi=180^\circ$ . Scattering angle in water is indicated as  $\Theta$  in the titles. Only three  $\gamma_b$  values are shown for clarity. The relative azimuth angle  $\Delta\phi$  is defined as the angular difference between sensor azimuth angle and solar azimuth angle. Thus,  $\Delta\phi=0^\circ$  if the sensor views along the retro-reflecting direction and  $\Delta\phi=180^\circ$  viewing along the mirror-reflecting direction.**

### Modeling error

More  $R_{rs}$  data are prepared by the same simulation code to assess the model error. Details of the simulation conditions are described in [Park and Ruddick, 2004]. In brief, the IOPs i.e.  $a$ ,  $b$  and SPFs were constructed with realistic ranges of  $Chl$ ,  $a_{CDOM}(443)$  (colored dissolved organic matter absorption at 443 nm) and  $b_{NC}(550)$  (scattering coefficient at 550 nm due to non-covarying particles). Wavelength varies from 412 to 780nm,  $Chl$  from 0.03 to 30 mg/m<sup>3</sup> and  $b_{NC}$  from 0 to 37 m<sup>-1</sup>. This dataset covers the  $a$  and  $b$  ranges typical of most case 1 and case 2 waters and differs from the simulated dataset used to calibrate the coefficients in Eq. (2) because non-discrete values are used, thus testing the model fitting

For given wavelength,  $Chl$ ,  $a_{CDOM}(443)$  and  $b_{NC}(550)$  give  $a$ ,  $b$  and  $b_b$ , which are converted to the  $X$  and  $\gamma_b$  parameters. Also, since the SPFs for covarying and non-covarying particles are represented by combination of  $P_{FF1}$  and  $P_{FF2}$  components according to backscatter ratio, the value of  $r_{FF1}$  can be obtained. Then with these  $X$ ,  $\gamma_b$  and  $r_{FF1}$  values, the simulated  $R_{rs}$  can be compared with the model described in the previous section. Figure 3 shows an example of the errors between simulation and model. The relative error is normally less than 1% and well within 2%, which is more accurate than the model which doesn't include the  $r_{FF1}$  parameter as input [Park and Ruddick 2004]. These errors vary with sun and sensor angles and increase slightly as scattering angle decreases or approaches 180°.

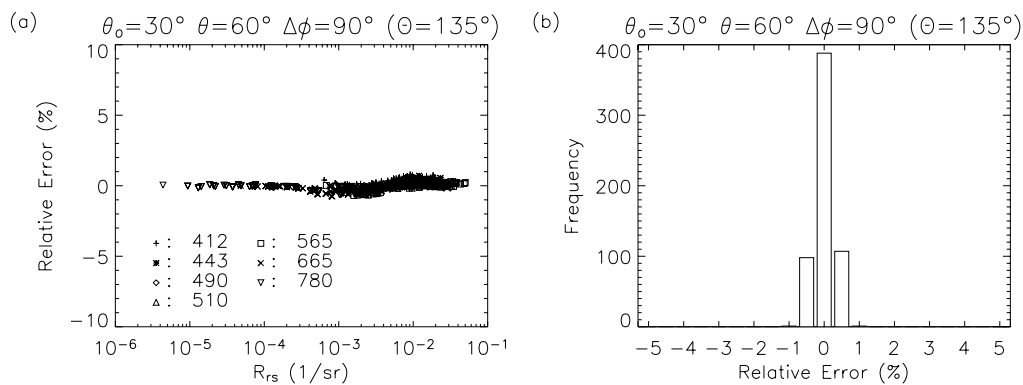


**Figure 3. Relative error of model from simulation**

### Remark for remote-sensing applications

The presented model requires two parameters  $\gamma_b$  and  $r_{FFI}$ , which can be computed from  $b_{bp}$  and  $Chl$  for given wavelength. If these parameters are available, as is possible for seaborne campaigns,  $R_{rs}(\theta_o, \theta, \Delta\phi)$  can be converted to the parameter  $X$ , which is an IOP, using the curves shown in Fig. 2. Then by applying the model again, the  $R_{rs}$  that would be measured at specific sun and sensor angles can be computed.

When these parameters are not known *a priori* as in satellite data processing, only an iterative technique could be adopted as suggested in [Loisel and Morel, 2001]. In reality, it could be difficult to achieve convergence to the target values for both  $Chl$  and  $b_{bp}$  simultaneously. However, considering that the realistic  $r_{FFI}$  variability is rather restricted for a given  $X$ , it would be practical to iterate only for the  $\gamma_b$  (equivalently  $b_{bp}$ ) with  $r_{FFI}$  (equivalently  $Chl$ ) fixed. After  $\gamma_b$  is determined by the iteration steps, the estimation of  $Chl$  gives the value of  $r_{FFI}$ , and finally with these  $\gamma_b$  and  $r_{FFI}$ , the bidirectional effect can be estimated.

### Summary and conclusions

A remote-sensing reflectance model has been presented, taking account of bidirectionality in case 1 and case 2 waters. This model requires  $r_{FFI}$  and  $\gamma_b$  as the model input. These parameters can be obtained from particle backscattering coefficient ( $b_{bp}$ ) and the chlorophyll concentration ( $Chl$ ) with the backscatter ratios for covarying and non-covarying particles.

Higher  $\gamma_b$  (corresponds to higher particle contribution to backscatter) gives higher  $R_{rs}$  for given particle SPF and  $X$ , although the opposite is observed for small  $X$  when scattering angle ( $\Theta$ ) is close to  $180^\circ$ . Lower  $r_{FFI}$  (higher backscattering from phytoplankton particles than from non-covarying particles) yields higher  $R_{rs}$  for given  $X$  and  $\gamma_b$ , although the difference is small for small  $X$  and  $\Theta$  close to  $180^\circ$ .

The difference between the model prediction and simulated  $R_{rs}$  is typically less than 1-2%, which seems suitable for describing the bidirectional variation.

It is important to demonstrate the application of this model to seaborne or satellite measurements. Especially, a realistic approach e.g. an iterative technique should be implemented for satellite data applications in the future.

The proposed model has not been validated by field measurements. Finally, the scattering phase functions for particles assumed in this study should be verified or updated in the future as better measurements become available.

### Acknowledgements

This study was supported by the Belgian Science Policy Office's STEREO programme in the framework of the BELCOLOUR project SR/00/03 and by PRODEX contract 15190/01.

## References

- Fournier, G. and J.L. Forand, Analytic phase function for ocean water, in *Ocean Optics XII*, J.S. Jaffe, ed., *Proc. SPIE*, 2258 (194-201), 1994.
- Gordon, H.R., O.B. Brown, R.H. Evans, J.W. Brown, R.C. Smith, K.S. Baker, and D.K. Clark, A semianalytic radiance model of ocean color, *J. Geophys. Res.*, 93 (D9), 10909-10924, 1988.
- Loisel, H., and A. Morel, Non-isotropy of the upward radiance field in typical coastal (Case 2) waters, *Int. J. Rem. Sens.*, 22 (2 & 3), 275-295, 2001.
- Mobley, C.D., *Light and Water: Radiative Transfer in Natural Waters*, Academic, San Diego, Calif., 1994.
- Mobley, C.D., and L.K. Sundman, *Hydrolight 4.2 Technical Documentation*, Sequoia Scientific, Inc., Redmond, Wash., USA, 2001.
- Mobley, C.D., L.K. Sundman, and Emmanuel Boss, Phase function effects on oceanic light fields, *Appl. Opt.*, 41 (6), 1035-1050, 2002.
- Morel, A., and B. Gentili, Diffuse reflectance of oceanic waters: its dependence on Sun angles as influenced by the molecular scattering contribution, *Appl. Opt.*, 30 (30), 4427-4438, 1991.
- Morel, A., and B. Gentili, Diffuse reflectance of oceanic waters. II. Bidirectional aspects, *Appl. Opt.*, 32 (33), 6864-6879, 1993.
- Morel, A., and B. Gentili, Diffuse reflectance of oceanic waters. III. Implication of bidirectionality for the remote-sensing problem, *Appl. Opt.*, 35 (24), 4850-4862, 1996.
- Morel, A., D. Antoine, and B. Gentili, Bidirectional reflectance of oceanic waters: accounting for Raman emission and varying particle scattering phase function, *Appl. Opt.*, 41 (30), 6289-6306, 2002.
- Park, Y. and K. Ruddick, A model of remote-sensing reflectance including case 1 and case 2 waters, submitted in 2004.
- Petzold, T.J., Volume scattering functions for selected ocean waters, *Tech. Rep. SIO 72-78*, Scripps Institution of Oceanography, San Diego, Calif., USA, 1972.
- Press, W.H., S.A. Teukolsky, W.T. Vetterling, and B.P. Flannery, *Numerical recipes in C: the art of scientific computing*, 2nd ed., Cambridge University Press, New York, 1992.
- Twardowski, M.S., M. Boss, J.B. Macdonald, W.S. Pegau, a.H. Barnard, and J.R.V. Zaneveld, A model for estimating bulk refractive index from the optical backscattering ratio and the implication for understanding particle composition in case I and case II waters, *J. Geophys. Res.*, 106 (C7), 14,129-14,142, 2001.